# Tailored Field-Emission Property of Patterned Carbon Nitride Nanotubes by a Selective Doping of Substitutional N(sN) and Pyridine-like N(pN) Atoms

Zhigang Zhong, Ga In Lee, Chan Bin Mo, Soon Hyung Hong, and Jeung Ku Kang*

*Department of Materials Science and Engineering, Korea Advanced Institute of Science and Technology, Daejeon, 305-701, Republic of Korea*

*Received January 11, 2007*
*Revised Manuscript Received April 18, 2007*

Field emission (FE), a phenomenon in which electrons are extracted from the surface of materials through the solid-vacuum potential barrier by electron tunneling,[1] has attracted considerable attention recently because of its numerous applications such as microwave telecommunications,[2] electron sources for electron microscopy,[3] luminescence tubes,[4] electrodes in gas discharge tubes,[5] X-ray tubes,[6] back light units,[7] and other vacuum electronic devices. Among these applications, the field-emission display (FED) is a direct and important one.

One key in developing FED and other field emission-based devices is to choose proper materials so-called "cold cathodes" which are distinguished from hot cathodes on the basis of thermionic emission.[8] According to previous studies,[8−10] A carbon nanotube (CNT) with hollow cylindrical structures of rolled graphite sheets[11] was shown to be a good candidate for field-emission applications[12] because of its inborn high aspect ratio, excellent electrical and mechanical properties, and chemical inertness.

Doping[10,13,14] is an attractive way to tailor carbon nanotubes (CNTs) with the significantly enhanced electron transport and emission properties. Chan et al.[15] showed that the nitrogen doping enhances the electron field-emission properties and Ahn et al.[16] theoretically estimated field-emission currents from nitrogen-doped single-walled (5,5) carbon nanotubes. It is considered that the atomic configurations of doped nitrogen atoms in these theoretical and experimental works involve only sN doping. On the other hand, the experimental process to dope N atoms into nanotubes usually introduces substitutional nitrogen (sN doping) and pyridine-like nitrogen (pN doping) atoms simultaneously. Here, we report that the sN-doping increases the FE performance by providing sufficient channels around the Fermi level, whereas the pN doping reduces the FE, thus indicating that the best approach to tailor nanotubes for enhancement of FE would be to maximize sN states by removing pN states.

To reveal the origin of sN and pN doping influences on the FE properties, we report here the first-principle calculation results on the basis of density functional theory (DFT) and matrix Green's function (MFG). Moreover, by experimentally changing the nitrogen doping level of carbon nitride nanotubes, we could change the FE performance of the devices because they have different amounts of sN type and pN type N atoms simultaneously, which could enhance or deteriorate the FE properties. In this respect, we have made the carbon nitride nanotubes with various nitrogen doping levels and performed various levels of analysis to identify the fundamental physics and chemistry responsible for the FE properties of nanotubes.

In this study, for the first-principle matrix Green's function (MGF) calculations, a semiconducting (10,0) CNT and a (6,6) metallic CNT were chosen as the models for study. The electric current is confined at the outermost shell of a capped multiwalled CNT in most cases,[17−18] thus capable of being effectively modeled as a single-walled CNT with the largest diameter having either a metallic or a semiconducting property depending on its chirality.[19−20] In this respect, we chose these two models in elucidating nitrogen doping effects on field emission performance of nanotubes. Two types of doping geometries, i.e., the sN doping and the pN doping, were proposed to model the nitrogen incorporation into pristine CNTs.[21] Figure 1a−c shows the geometries of the pristine, sN-doped, and pN-doped (10, 0) nanotube, respectively. Similarly, Figure 1d−f demonstrates those cases of the metallic (6,6) nanotube. All of these geometries of nanotubes are optimized using the Perdew−Burke−Enzhrof scheme generalized gradient approximation (GGA).[22] The

* Corresponding author. E-mail:jeungku@kaist.ac.kr.

(1) (a) Fowler, R. H.; Nordheim L. *Proc. R. Soc. London, Ser. A* **1928**, *119*, 173. (b) Gadzuk J. W.; Plummer E. W. *Rev. Mod. Phys.* **1973**, *45*, 487.
(2) Teo, K. B. K.; Minoux, E.; Hudanski, L.; Peauger, F.; Schnell, J. P.; Gangloff, L.; Legagneux, P.; Dieumegard, D.; Amaratunga, G. A. J.; Milne, W. I. *Nature* **2005**, *437*, 968.
(3) de Jonge, N.; Lamy, Y.; Schoots, K.; Oosterkamp, T. H. *Nature* **2002**, *420*, 393.
(4) Bonard, J. M.; Stockli, T.; Noury, O.; Chatelain, A. *Appl. Phys. Lett.* **2001**, *78*, 2775.
(5) Rosen, R.; Simendinger, W.; Debbault, C.; Shimoda, H.; Fleming, L.; Stoner, B.; Zhou, O. *Appl. Phys. Lett.* **2000**, *76*, 1668.
(6) Yue, G. Z.; Qiu, Q.; Gao, B.; Cheng, Y.; Zhang, J.; Shimoda, H.; Chang, S.; Lu, J. P.; Zhou, O. *Appl. Phys. Lett.* **2002**, *81*, 355.
(7) Lee, S.; Im, W. B.; Kang, J. H.; Jeon, D. Y. *J. Vac. Sci. Technol., B* **2005**, *23*, 745.
(8) Xu, N. S.; Huq E., *Mater. Sci. Eng., R* **2005**, *48*, 47.
(9) Bonard, J. M.; Kind, H.; Stockli, T.; Nilsson, L. O. *Solid State Electron.* **2001**, *45*, 893.
(10) Zhou, G.; Duan, W. J. *Nanosci. Nanotechnol.* **2005**, *5*, 1421.
(11) Iijima, S. *Nature* **1991**, *354*, 56.
(12) de Heer, W. A.; Bonard, J. M.; Fauth, K.; Chatelain, A.; Forro, L.; Ugarte, D. *Adv. Mater.* **2004**, *9*, 87.
(13) Zhang, G.; Duan, W.; Gu, B. *Appl. Phys. Lett.* **2002**, *80*, 2589.
(14) Charlier, J. C.; Terrones, M.; Baxendale, M.; Meunier, V.; Zacharia, T.; Rupesinghe, N. L.; Hsu, W. K.; Grobert, N.; Terrones, H.; Amaratunga, G. A. *Nano Lett.* **2002**, *2*, 1191.
(15) Chan, L. H.; Hong, K. H.; Xiao, D. Q.; Hsieh, W. J.; Lai, S. H.; Shih, H. C.; Lin, T. C.; Shieu, F. S.; Chen, K. J.; Cheng, H. C. *Appl. Phys. Lett.* **2003**, *82*, 4334.
(16) Ahn, H. S.; Lee, K. R.; Kim, D. Y.; Han, S. *Appl. Phys. Lett.* **2006**, *88*, 093122.
(17) Frank, S.; Poncharal, P.; Wang, Z. L.; de Heer, W. A. *Science* **1998**, *280*, 1744.
(18) Bachtold, A.; Strunk, C.; Salvetat, J. P.; Bonard, J. M.; Forro, L.; Nussbaumer, T.; Schonenberger, C. *Nature* **1999**, *397*, 673.
(19) Saito, R.; Fujita, M.; Dresslhaus, G.; Dresslhaus, M. S. *Appl. Phys. Lett.* **1992**, *60*, 2204.
(20) Ebbesen, T. W.; Lezec, H. J.; Hiura, H.; Bennett, J. W.; Thio, T. *Nature* **1996**, *382*, 54.
(21) Sun, C. L.; Wang, H. W.; Hayashi, M.; Chen, L. C.; Chen, K. H. *J. Am. Chem. Soc.* **2006**, *128*, 8368.
(22) Perdew, J. P.; Burke, K.; Ernzerhof, M. *Phys. Rev. Lett.* **1996**, *77*, 3865.

10.1021/cm070099+ CCC: $37.00 
Published on Web 05/19/2007

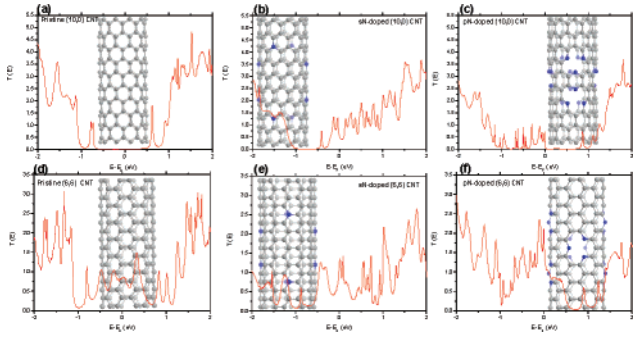

**Figure 1.** Transmission coefficients obtained from (a) pristine (10,0), (b) substitutional N-doped (10,0), (c) pyridine-like N-doped (10,0), (d) pristine (6,6), (e) substitutional N-doped (6,6), and (f) pyridine-like N-doped (6,6) nanotubes.

FE phenomenon is a kind of electron transmission under extrinsic electric field. To apply the voltage to the nanotubes, they are sandwiched between two semi-infinite electrodes.[23] We have then determined the electronic structures for the sandwiched nanotube using 2D (dimensional) DFT calculations with the PBE functional and a norm-conserving pseudopotential.[24−26] (Refer to the Supporting Information for details.)

As shown in Figure 1a, the highest occupied molecular orbital (HOMO) and the lowest unoccupied molecular orbital (LUMO) are separated by an ∼1.5 eV energy gap for a semiconducting pristine nanotube. On the other hand, in the sN-doped nanotube as shown in Figure 1b, the HOMO state becomes higher than that of a pristine nanotube by 0.7 eV. Meanwhile, many unoccupied states, including the LUMO state, are created from nonbonded electron pairs of nitrogen. These HOMO state and unoccupied states make many channels near the Fermi energy, which allows for a high transmission coefficient and makes the sN-doped nanotube a good conductor. On the other hand, although there are many occupied states near the Fermi energy in a pyridine-type N-doped nanotube, the energy levels of the unoccupied states are too high, which results in a high band gap and gives a negligible transmission coefficient. Figure 1d−f indicatea that the (6,6) nanotube remains metallic after sN doping and pN doping. On the other hand, it is determined that new channels are added at unoccupied states when sN doping is included, shown in Figure 1e. However, it is found that the channels at unoccupied states near the Fermi energy become destroyed compared to the pristine (6,6) case when pN doping is included, shown in Figure 1f. In this respect, it is concluded that new channels are created in the unoccupied band for both the semiconducting and metallic nanotubes when sN doping is included, whereas the channel states for a semiconducting nanotube and a metallic nanotube become depleted when pN doping is included. These results indicate that sN doping rather than pN doping should be increased in nanotubes to improve the field emission of CNT arrays.

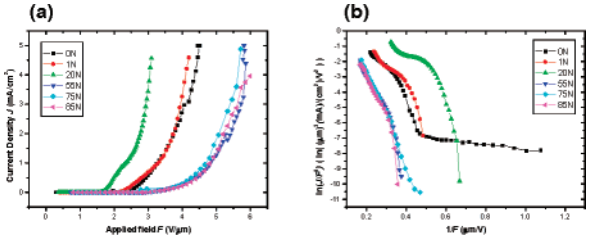

**Figure 2.** (a) Field-emission $J-F$ plot obtained from six samples with different N concentrations of 0N, 1N, 20N, 55N, 75N, and 85N, and (b) their corresponding Fowler−Nordheim plot.

**Table 1. Field-Emission Properties of the Samples with Different Nitrogen Concentrations**[a]

| | 0N | 1N | 20N | 55N | 75N | 85N |
|---|---|---|---|---|---|---|
| turn-on | 2.2 | 2.1 | 1.6 | 2.9 | 3.0 | 3.0 |
| threshold | 3.3 | 3.3 | 2.3 | 4.8 | 4.7 | 4.8 |

[a] Electric field unit is V/$\mu$m.

Also, the carbon nanotubes for the FED were synthesized by PECVD on TiN-coated Si substrates using Co thin film as catalyst and $CH_4$ and $H_2$ and/or $N_2$ as flowing gases. To control the nitrogen doping level, we varied the $N_2$ concentration of the flowing gases[27] from 0 to 85%, as summarized in the Supporting Information. Accordingly, the samples were named 0N, 1N, 20N, 55N, 75N, and 85N. After the PECVD process, patterned black dots (0.2 mm × 0.2 mm) appeared on the substrate over a 1 cm$^2$ area as arrays (Figure 2a). Scanning electronic microscopy (SEM) and transmission scanning electronic (TEM) images confirm that these dots are composed of close-packed vertically aligned nanotubes (see the Supporting Information).

The applied field-emission−current-density ($F-J$) relations and corresponding Fowler−Nordheim plots are given in Figure 2. Here, two major parameters are employed to examine the field-emission performance from different samples: The first parameter is the turn-on field, defined as the applied field to achieve the current density of 10 $\mu$A/cm$^2$. The second parameter is the threshold field, defined as the applied field to achieve the current density of 1 mA/cm$^2$. These parameters for all the samples studied are summarized in Table 1. The FE performances of these samples can be divided into three groups: the first case is the sample 20N, which shows the lowest turn-on and threshold fields of 1.6 and 2.3 V/$\mu$m, respectively. Meanwhile, samples 0N and 1N show intermediate turn-on and threshold fields of ∼2.1 and 3.3 V/$\mu$m, respectively. The last case is for samples 55N, 75N, and 85N, which show the highest turn-on and threshold fields of ∼3.0 and 4.8 V/$\mu$m, respectively. These results indicate that there is an optimal nitrogen concentration (20N) between the lowest (0N) and the highest (85N) nitrogen doping levels to achieve the best field-emission performance.

In addition, XPS was applied to confirm the nitrogen configurations in our prepared nitrogen-doped nanotubes. As shown in Figure 3, the N 1s XPS spectra can be divided by three Lorentz fits: 398.2 eV corresponds to nitrogen substitution of one carbon atom in a single benzene ring,[28]

(23) Schults, P. *SeqQuest Project*; Sandia National Laboratories: Albuquerque, NM, 2003.
(24) Hamann, D. R. *Phys. Rev. B* **1989**, *40*, 2980.
(25) Troullier, N.; Martins, J. L. *Phys. Rev. B* **1991**, *43*, 1993.
(26) Kim, Y.-H.; Jang, S. S.; Jang, Y. H.; Goddard, W. A. *Phys. Rev. Lett.* **2005**, *94*, 156801.
(27) Jang, J. W.; Lee, C. E.; Lyu, S. C.; Lee, T. J.; Lee, C. J. *Appl. Phys. Lett.* **2004**, *84*, 2877.
(28) Stafstrom, S. *Appl. Phys. Lett.* **2000**, *77*, 3941.

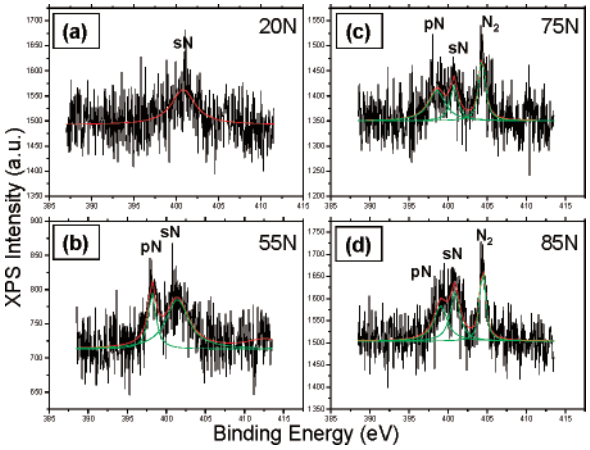


**Figure 3.** XPS spectra obtained from the four samples with different nitrogen concentrations of (a) 20N, (b) 55N, (c) 75N, and (d) 85N.

the combination of which can form a pyridine-like carbon nitride structure (pN); 401.3 eV corresponds to nitrogen substitution of one carbon atom in a graphite-like carbon network (sN);[29] and 404.8 eV corresponds to the physically adsorbed molecular $N_2$, where the binding energy of 404.8 eV is lower than the original binding energy of 409.9 eV for the free $N_2$ gas, attributed to the screening effect between N 1s core hole and matrix.[30] There is only one sN peak obtained from the sample 20N (Figure 3a). On the other hand, as the N concentration increases, we find that a pN peak along with the sN peak shows up from sample 55N (Figure 3b). The further increase in nitrogen brings additional $N_2$ peaks in samples 75N and 85N (panels c and d in Figure 3). These results give the important implication: when the sN doping is done, FE is enhanced compared to a pristine carbon nanotube. However, as the N concentration further increases, pyridine-like nitrogen doping occurs and the FE current density decreases. In this respect, a proper nitrogen doping level is necessary to achieve the best FE performance, as it could only create the sN doping by preventing the pN doping.

On the basis of our first-principle calculations and experiments mentioned in the above, our results can be explained like this: when the supply of nitrogen during nanotube formation is rare (such as in sample 20N), the sN doping with lower amounts of nitrogen is more likely to occur than the pN doping, as experimentally supported by XPS analysis (Figure 3a). However, as the nitrogen supply is increased, pN type nitrogen configurations also increase, as observed in the experimental results shown in Figure 3b−d, which were obtained from samples 55N, 75N, and 85N, respectively. As a result, sample 20N, which includes only substitutional nitrogen, shows the better field-emission (FE) performance because of the increased number of free electrons compared to that for the pristine CNT (0N), whreas samples such as 55N, 75N, and 85N show worse FE performance than those for the 0N and the 20N because of the reduction of free electrons.

In conclusion, the FE performance of nitrogen-doped carbon nitride nanotubes with different sN-and pN-nitrogen levels were studied by both first-principle calculations and experiments. The field emission current can be reduced by heavy doping. The first-principles matrix Green's function calculations reveal that the sN doping, which is likely to happen when the nitrogen supply is moderate, can increase the number of free electrons in a nanotube. However, it is found that pN doping, which is more likely to happen when the nitrogen supply is plentiful, decreases the numbers of free electrons in nanotube. The finding implies that the control of sN-doping and pN-doping states in carbon nanotubes is critical to enhancing the FE performance. Also, the nitrogen configuration level in nanotubes was controlled by the nitrogen concentration in flowing gases. Experimental results indicate that an optimal amount of nitrogen doped into nanotubes can improve their field-emission performance. In this respect, the best approach to tailor nanotubes for enhancement of FE would be to maximize sN-doping states with elimination of pN states.

**Acknowledgment.** This work was supported by the interdisciplinary research program and CUPS sponsored by KOSEF (KOSEF-R01-2005-000-10330-0) and Grant M103KW010017-06K2301-01720 from the Hydrogen Energy R & D program of the Ministry of Science & Technology.

**Supporting Information Available:** Green function compution, synthesis procedures, SEM and TEM images (PDF). This material is available free of charge via the Internet at http://pubs.acs.org.

CM070099+

(29) Souto, S.; Pickholz, M.; dos Santos, M. C.; Alvarez, F. *Phys. Rev. B* **1998**, *57*, 2536.
(30) Esaka, F.; Shimada, H.; Imamura, M.; Matsubayashi, N.; Kikuchi, T.; Furuya, K. *J. Electron Spectrosc. Relat. Phenom.* **1998**, *88−91*, 817.